Self-consistent simulations of nanowire transistors using atomistic basis sets

Neophytos Neophytou, Abhijeet Paul, Mark S. Lundstrom, and Gerhard Klimeck

Purdue University, School of Electrical and Computer Engineering,
Network for Computational Nanotechnology, West Lafayette, IN, USA

{neophyto|paul1|lundstro|gekco}@purdue.edu

Abstract

As device sizes shrink towards the nanoscale, CMOS development investigates alternative structures and devices. Existing CMOS devices will evolve from planar to 3D non-planar devices at nanometer sizes. These devices will operate under strong confinement and strain, regimes where atomistic effects are important. This work investigates atomistic effects in the transport properties of nanowire devices by using a nearest-neighbor tight binding model ($sp^3s^*d^5$-SO) for electronic structure calculation, coupled to a 2D Poisson solver for electrostatics. This approach will be deployed on nanoHUB.org as an enhancement of the existing Bandstructure Lab.

Introduction-Approach

The 2D cross section of a 3D device is described with an arbitrary geometrical shape such as rectangular, cylindrical and tri-gate/FinFET type of structures (Fig. 1(a-d)). A finite element mesh enables the treatment of extended device components and includes the atomic locations in the interior semiconductor. The electronic structure in a nanowire channel is described in an atomistic representation using a 20 orbital nearest-neighbor tight binding model ($sp^3s^*d^5$-SO) [1]. A nanowire with a given cross section and transport orientation is specified, and its corresponding bandstructure is calculated using the unit cell information, based on the underlying atomic lattice (Fig. 1e). To account for any changes to the bandstructure due to potential and charge variations in the wire, the electronic structure is calculated self-consistently with a Poisson solution for the electrostatic potential in the cross section. Upon potential convergence of the infinite wire, the ballistic transport characteristics are calculated with a semi-classical ballistic model (Fig. 1f) [2].

Results - Discussion

Figure 2 shows the self consistent results for the charge distribution in a 3nm x 3nm square, [100] transport direction, Si nanowire, under low and high gate bias conditions, i.e. when the channel is partially and fully inverted. The underlying structure of the atoms is evident in the case where the channel is fully inverted (dots).

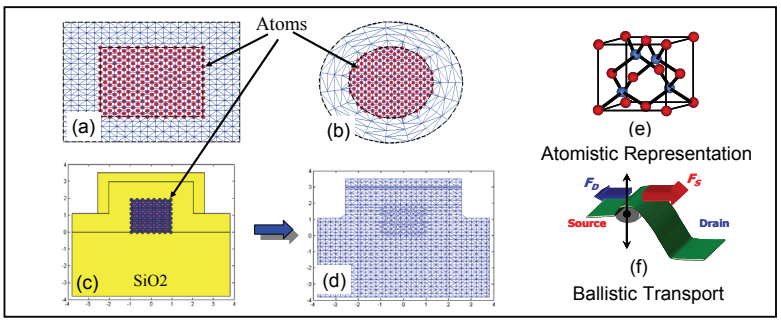

Figure 1: The 2D cross sections of the devices treated. The finite element mesh and the atomic positions (dots) are indicated. (a) Rectangular, (b) Cylindrical, (c) The tri-gate device structure, (d) The mesh for the tri-gate structure. (e) The zincblende lattice configuration used for the atomistic description of the device. (f) The semi-classical ballistic model used to calculate device characteristics.

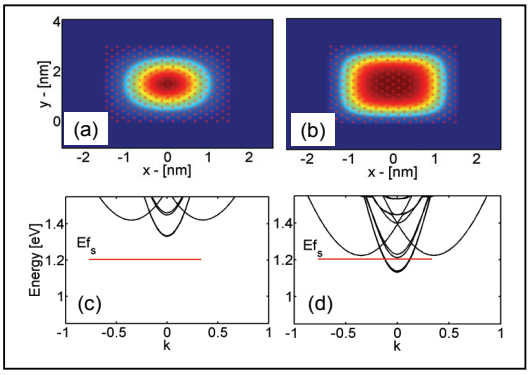

Figure 2: Device features for a 3nm rectangular wire. (a-b) The 2D cross section showing the charge distribution under low and high gate biases, respectively. The dots indicate the underlying atomic positions. (c-d) E(k) plots for the cases (a-b). Ef_s is the source Fermi level.

A nanowire dispersion curve is usually considered to be a material and geometry dependent quantity, independent of the filling of the states. The difference between Fig. 2c-d, however, indicates that the dispersion in Fig. 2d is not a solid shift in energy from Fig. 2c. The first set of excited states shifts below the bandedge minima at k=0.45. The filling of the states in the device changes the electrostatic potential, which in turn changes the lateral confinement. The change in the lateral confinement in turn changes the dispersion in the transport direction. Larger nanowires show another interesting behavior under inversion conditions. With increasing gate biases the charge shifts from being confined in the center of the wire to be confined in the corners of the wire. The electrostatics of the device force these corner regions into stronger inversion (Fig. 3a,b). Figures 3c-d also shows significant changes in the bandstructure of the nanowire between the low and high bias conditions cases.

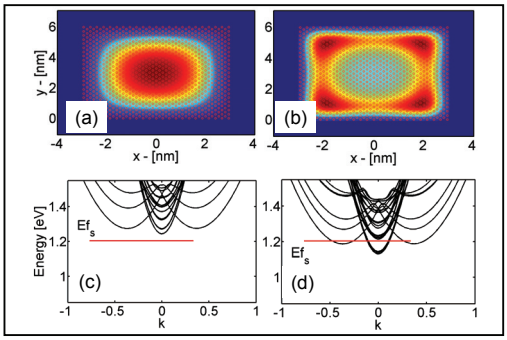

Figure 3: Device features for a 6nm rectangular wire. (a-b) The 2D cross section showing the charge distribution under low and high gate biases, respectively. The dots indicate the underlying atomic positions. (c-d) The corresponding E(k) plots for the cases (a-b). Ef_s is the source Fermi level.

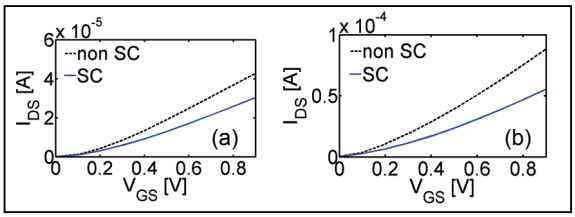

Figure 4: The I_D-V_G characteristics calculated using the empty (non-SC) E(k) diagram and using the charge filled (SC) E(k) diagram for the 3nm and 6nm rectangular nanowires. (a) The 3nm device. (b) The 6nm device.

Changes in the bandstructure and spatial distribution of charges reflect on the I-V device characteristics. Figure 4 shows a comparison between the I_D-V_G characteristics of the device for two simulation approaches: (i) the Poisson equation is solved in the cross section of the rectangular nanowire and the potential variation is considered in the bandstructure calculation, and (ii) a simple planar capacitance (oxide capacitance) is considered for the electrostatics of the device (no potential variation is considered in the cross section). The spatial variation of the charge, however, (i.e. volume inversion for small wires) makes the simple capacitance assumption inaccurate. This, together with the variation of the E(k) levels through self-consistency (larger wires), result in significant differences in the I_D-V_G characteristics obtained by the two methods, for both, small 3nm diameter (Fig. 4a), and larger, 6nm diameter (Fig.4b) wires. Considering only a simple shift of the bands due to the gate bias will result in overestimating the drive current of the device. This observation can be different for different device shapes and sizes however. It is noted here that in all the calculations the potential variations between the atomic locations in the wire are small compared to the tight-binding parameters used, so the tight-binding approximation is still valid.

The Poisson solution on a 3D zincblende lattice poses an interesting challenge for typical regular mesh solvers, zincblende is not a space-filling mesh. The lattice can be symmetrised and solved in standard finite difference methods in 3D (Fig. 5a). The 2D solution corresponds in a 3D representation to Fig. 5b indicating that the 2D

approximation spreads out charge in real space significantly different than the original zincblende lattice. The differences in the I-V characteristics between the two methods for this particular case can be up to 10%. However, the 3-D solution is computationally much more expensive than the 2D solution (Fig. 5c). Depending on the discretization of the mesh and the k-space resolution in the bandstructure calculation, the Poisson solution in 3D can account for a large part of the total computation time for little difference in the results, so we typically utilize the 2D Poisson solution.

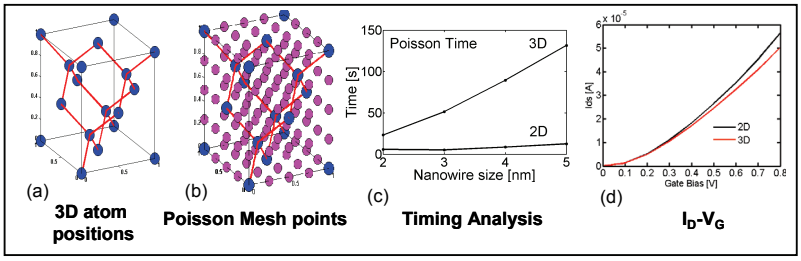

Figure 5: (a) The position of the atoms in the zincblende lattice. (b) 3D mesh nodes for the equivalent 2D Poisson. (c) Time comparison between a full 3-D atomistic lattice and a quasi 2-D solution. (d) I_D-V_G characteristics computed for quasi 2-D and full 3-D Poisson solution.

Conclusions

A tight binding approach is used to calculate the electronic structure of nanowire devices self consistently with a 2D Poisson equation. Using a semi-classical ballistic model, the transport characteristics are then evaluated. Atomistic effects and an accurate description of the electronic structure are important features and need to be taken into consideration when computing transport characteristics of nanoscale devices. A 2D Poisson solution is found to be sufficient compared to a full 3D Poisson solution for infinite wires. The solution methods are fast enough to rapidly explore device configurations. This work will enhance to the Bandstructure Lab tool [3] that is already freely accessible on nanoHUB.org.

Acknowledgements

This work was supported by the Semiconductor Research Corporation (SRC) and Microelectronics Advanced Research Corporation (MARCO). nanoHUB.org computational resources were used in this work.

References

[1] G. Klimeck, F. Oyafuso, T. B. Boykin, R. C. Bowen, and P. von Allmen, Computer Modeling in Engineering and Science (CMES) Volume 3, No. 5 pp 601-642 (2002).
[2] A. Rahman, J. Guo, S. Datta, and M. Lundstrom, IEEE TED, 50, pp. 1853-1864, 2003.
[3] Bandstructure lab on nanoHUB.org (https://www.nanohub.org/tools/bandstrlab/)